

Modification of the Magnetic Field Structure in the Vicinity of the *X-Point* by the Strong Mirror Field for a Field-Reversed Configuration (FRC) with the Thick *Edge-Layer* Plasma

SUZUKI Yukihiisa, OKADA Shigefumi¹ and GOTO Seiichi¹

*Department of Electronics and Information Engineering, Graduate School of Engineering,
Tokyo Metropolitan University, 1-1 Minami Oosawa, Hachioji, Tokyo 192-0397, Japan*

¹ *Plasma Physics Laboratory, Graduate School of Engineering, Osaka University,
Yamada-Oka 2-1, Suita, Osaka 565-0871, Japan*

(Received: 11 December 2001 / Accepted: 6 September 2002)

Abstract

Modification of the magnetic field structure in the vicinity of the *x-points* and changes of the separatrix shape are investigated under the pressure effects due to an *edge-layer* plasma together with a mirror field by the two-dimensional (2-D) MHD equilibrium solutions of field-reversed configuration (FRC) obtained from the Grad-Shafranov equation. To explore the coupling pressure effects caused by *edge-layer* plasma and mirror field, the equilibrium calculations are performed by the combinations of several values of mirror ratio (R_m) and of *edge-layer* width (δ), respectively. A summary of results for present study is as follows. In the condition of weak mirror field ($1.0 < R_m < 1.6$), $\psi=0$ surface opens up in the axial direction, namely 2-D FRC equilibrium with closed separatrix is lost when δ is above the critical value. When the mirror field is strong enough as $R_m > 1.6$, $\psi=0$ surface never opens up for any δ . These original results make it clear that large magnetic curvature produced by the strong mirror field enhances the magnetic stress around the *x-point*, so that the ends of FRC are effectively sustained by this enhanced magnetic stress, which counteracts the *edge-layer* plasma pressure effect.

Keywords:

FRC, MHD equilibrium, Grad-Shafranov equation, mirror field, *edge-layer* plasma, axial force balance

1. Introduction

A field-reversed configuration [1,2] (FRC) is an axisymmetric elongated compact toroid with negligible toroidal magnetic field. It has an extremely high average β value which reaches 0.9 or higher [3]. Here the value of β is the ratio of the plasma pressure to the external magnetic pressure. Because of such a characteristic, FRC plasma is thought to be influenced by the change of external magnetic field and the *edge-layer* plasma.

Previously, there were a few studies in which *edge-layer* effects were taken into account [4-6]. The relation between the separatrix shape and the thickness of the

edge-layer plasma is shown in ref. 5. In this study, it is found that $\psi=0$ surface opens and the closed 2-D FRC equilibrium is lost when the thickness increases further. Here, $\psi(r,z)$ denotes poloidal magnetic flux function, and closed $\psi=0$ surface corresponds to separatrix in ordinary FRC equilibria. In ref. 6, the dependence of the separatrix shape on β_s is shown. Here β_s denotes the local β value on the separatrix. This study indicates that axial pressure balance does not hold unless $\psi=0$ surface opens up, as the value of β_s is above the critical value.

Corresponding author's e-mail: suzuki@eei.metro-u.ac.jp

©2002 by The Japan Society of Plasma
Science and Nuclear Fusion Research

There have been some measurements and discussion of the edge-layer plasma [7-10]. In ref. 7 plasma density was measured and found to extend outside the separatrix to form the *edge-layer*. More directly, in a recent study on the FRC Injection Experiment [11] (FIX) at Osaka University, the thickness of the *edge-layer* plasma is inferred from the plasma pressure to be approximately 30~40 % of the separatrix radius [12]. A feature of the FRC confined in the FIX machine is the existence of a large mirror ratio as $R_m=2\sim 8$ at both ends. The value of R_m denotes the ratio of the magnetic field strength in the mirror region to that in the midplane without the FRC plasma. In this study, the terms of "strong mirror field" or "large mirror ratio" are used to refer to $R_m \geq 2.0$, which indicates the operation parameter of FIX. The terms of "weak mirror field" or "small mirror ratio" indicate the condition of $1.0 \leq R_m < 2.0$, which is used most of other FRC device. It is expected that a high *edge-layer* pressure can be sustained by a strong mirror field. However, in the previous numerical studies, a strong mirror field has not been considered as to its effects on the *edge-layer*.

In this paper, the following new results are found as for those coupling pressure effects by 2-D numerical MHD equilibria. In the case of strong mirror condition as $R_m \geq 1.6$, $\psi=0$ surface never opens up for any *edge-layer* plasma width. Since the magnetic stress around the *x-point* is enhanced by large magnetic curvature due to the strong mirror field, the ends of FRC are effectively sustained no matter how the *edge-layer* plasma pressure effect is large.

2. Numerical Method

The effect of the *edge-layer* plasma on the equilibria is investigated using a previously developed 2-D numerical MHD equilibrium code [13]. In this code, the Grad-Shafranov equation without toroidal field is solved to obtain the equilibrium solution. The equation is written in the cylindrical coordinate system (r, θ, z) as follows:

$$\Delta^* \psi = -r^2 \frac{dp(\psi)}{d\psi}, \quad (1)$$

where

$$\Delta^* = r \frac{\partial}{\partial r} \left(\frac{1}{r} \frac{\partial}{\partial r} \right) + \frac{\partial^2}{\partial z^2}.$$

Here, ψ is the poloidal flux function and $p(\psi)$ denotes the scalar pressure profile function which depends only on ψ . To obtain thin and elongated equilibria as given in the experimental data of FIX, $p(\psi) = -c(\psi + 1/2\epsilon\psi^2)$ is

appropriate as the pressure model [13]. The recent FIX experiment [12] shows that an exponentially decaying pressure profile is suitable to represent the equilibrium in the open field region. It is required that the current

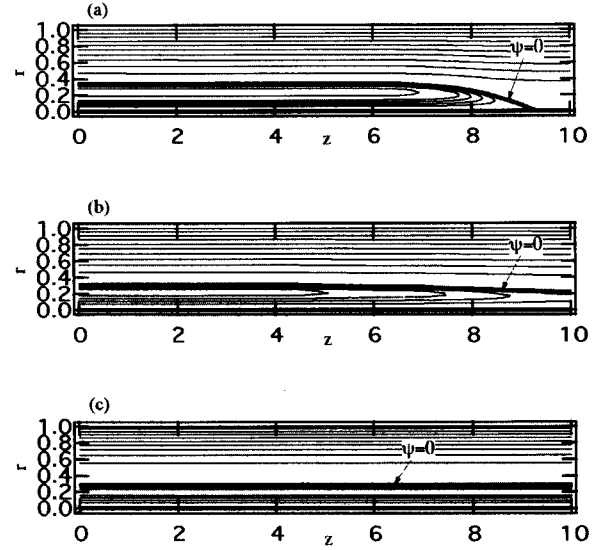


Fig. 1 A series of FRC equilibria for $S_0=2.6$, $R_m=1.0$ and $\epsilon=40.0$: (a) $\gamma=30.0$; (b) $\gamma=20.0$; (c) $\gamma=2.0$. Contours of the poloidal flux function $\psi(r,z)$ are shown; contour intervals are 0.1 for $\psi>0$ and 0.002 for $\psi\leq 0$, respectively. The thick contour line denotes the surface $\psi=0$.

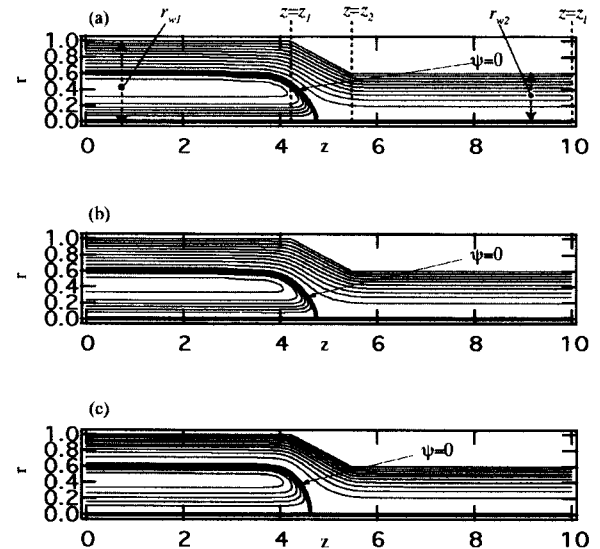


Fig. 2 A series of FRC equilibria for $S_0=2.6$, $R_m=2.8$ and $\epsilon=40.0$: (a) $\gamma=30.0$; (b) $\gamma=20.0$; (c) $\gamma=2.0$. Contours of the poloidal flux function $\psi(r,z)$ are shown; contour intervals are 0.1 for $\psi>0$ and 0.004 for $\psi\leq 0$, respectively.

density is continuous across the separatrix. For reasons mentioned above, we choose the following model as the pressure profile [14].

$$\frac{dp(\psi)}{d\psi} = \begin{cases} -c(1 + \varepsilon\psi) & (\psi \leq 0), \\ -ce^{-\gamma\psi} & (\psi > 0). \end{cases} \quad (2)$$

Here ε and γ are constant parameters, and c is an eigenvalue to be determined by the global constraint that is the area (S_0) inside of the separatrix. This global constraint is necessary to obtain non-trivial solutions, since the solution of the eigenvalue equation derived from eq. (1) generally gives a variety of FRC equilibria. The separatrix radius can be controlled by ε as described in ref. 15. When ε is larger, the separatrix radius becomes smaller. The pressure distribution in the *edge-layer* is governed by γ , which specifies the width of the edge plasma. An equilibrium with a thick *edge-layer* is produced by choosing small values for γ . Note that we define $\psi \leq 0$ inside the separatrix and $\psi > 0$ outside the separatrix.

The boundary conditions are as follows: $\psi=0$ at $r=0$, $\partial\psi/\partial z=0$ at $z=0$ and $z=z_1$, and $\psi=\psi_{\text{wall}}$ at the chamber wall (see Fig. 2(a)). In this paper ψ is normalized by ψ_{wall} . The mirror field is generated by reducing the wall radius r_{w2} at $z_2 < z < z_1$, because the flux is conserved inside the chamber wall as shown in Fig. 2 (a). Hence, the mirror ratio is given by $(r_{w1}/r_{w2})^2$.

3. Results

Numerical calculations are performed for the following cases: $R_m=1.0, 1.2, 1.6, 2.0$, and 2.8 . The range of variation of γ examined in this study is $1.0 \leq \gamma \leq 40.0$ for each value of R_m . The *edge-layer* thickness is changed from thick to thin by varying this parameter γ . The coordinate (r, z) is normalized by the wall radius r_{w1} in this study. The cross-sectional area S_0 inside of the separatrix is calculated under that metric. The global constraint S_0 determines the separatrix length l_s . When S_0 is larger, equilibrium with large l_s is obtained. To investigate the effect of mirror field, a long and thin equilibrium as $1/2 l_s \sim 9$ and $x_s \sim 0.4$ is needed in the condition of $R_m=1.0$, because mirror field is generated at $z > 4.3$. Here, l_s is the separatrix length normalized by x_s , and x_s is the ratio of the separatrix radius to the wall radius r_{w1} . For reasons stated above, the global constraint S_0 is fixed at 2.6 and the value of ε is chosen to be 40.0 in all of the calculations.

To investigate the dependence of the equilibrium shape on γ , the examples of the poloidal flux function

$\psi(r, z)$ are shown in Fig. 1 for $R_m=1.0$ and a variety of γ values. Figures (a), (b) and (c) correspond to $\gamma=30.0, 20.0$ and 2.0 , respectively. The separatrix surface, defined by $\psi=0$, is denoted by a bold line. When $\gamma=30.0$, the $\psi=0$ surface is closed, and a solution with elliptical separatrix shape is obtained. For the case of $\gamma=20.0$, however, the $\psi=0$ surface is open. When γ is 2.0, the solution becomes z -independent as shown in Fig. 1 (c). In the case of a thick *edge-layer*, $2 < \gamma < 20$, an equilibrium solution with closed $\psi=0$ surface cannot be obtained. The equilibrium shape is sensitive to the *edge-layer* pressure distribution, when $R_m=1.0$. In this case, the so-called *x-point* easily goes to infinity with increasing *edge-layer* thickness. These results are consistent with the previous study presented in refs. 5 and 6.

Equilibria with a strong mirror field, $R_m=2.8$, are shown in Fig. 2. In the same manner as above, Figs. 2(a), (b) and (c) correspond to $\gamma=30.0, 20.0$ and 2.0 , respectively. The $\psi=0$ surface does not open up in every case and the separatrix shape does not change much with this strong mirror case. The values of x_s and l_s change little in these three cases, which are $x_s \sim 0.61$ and $l_s \sim 9.4$. The separatrix length does not change much with the *edge-layer* thickness when the mirror ratio is large. It is found that the mirror field plays a significant role for the equilibrium, because with a large mirror ratio the equilibrium shape is independent of the *edge-layer* width compared with the case of $R_m=1$.

The approximate existence region of the equilibrium from this calculation is shown in Fig. 3. In

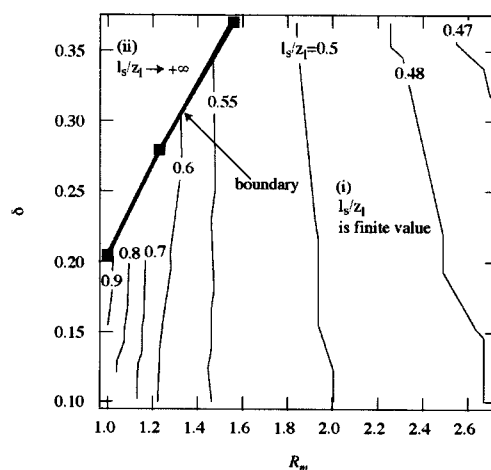


Fig. 3 The region in which 2-D FRC equilibria exist with respect to the parameters δ and R_m . The value of l_s/z_1 goes to $+\infty$ in region (ii). FRC equilibria can exist in region (i).

this figure, the vertical and the horizontal axes denote *edge-layer* width and R_m , respectively, and each line shows a contour of constant l_s/z_l . The *edge-layer* width is defined by δ at the mid-plane which satisfies $\beta(r_s+\delta)=e^{-1}\beta_s$. Here r_s satisfies $\psi(r_s,0)=0$, $\beta(r)$ denotes local beta value, and β_s denotes the $\beta(r)$ on the $\psi=0$ surface. When γ becomes smaller, *edge-layer* width δ increases. The value of δ is normalized by the wall radius in Fig. 3. The three square markers are critical values of δ_c calculated at each R_m . The bold line indicates the inferred boundary that divides the parameter region into one in which the value of l_s/z_l goes to $+\infty$ from that in which l_s/z_l is finite. Equilibria with closed $\psi=0$ surface cannot exist above and to the left of the bold line. In the weak mirror region, from $R_m=1.0$ to 1.6, the critical value of δ_c increases from 0.2 to 0.37 as R_m increases. In the parameter region of this figure ($\delta < 0.37$), the critical boundary disappears for $R_m > 1.6$. It is found that only a moderate mirror field is required to sustain the 2-D FRC equilibrium with a thick *edge-layer* of $\delta \sim 0.37$.

4. Modification of the Magnetic Field Near the X-Point

The details of the magnetic field structure and the axial force balance are examined to interpret the numerical equilibrium results. To investigate the magnetic structure of the FRC, we make a vector plot of the magnetic field \mathbf{B} around the end region. The magnitudes of the vectors are normalized by the absolute value of $\mathbf{B}(r_{w1},0)$. Figures 4(a) and (b) correspond to the conditions $R_m=1.2$, $\gamma=15.0$ and $R_m=2.8$, $\gamma=15.0$, respectively. These are the cases with a thick *edge-layer*. The regions surrounded with thin-lined circles are compared in both figures; the magnetic curvature is larger for $R_m=2.8$ than for $R_m=1.2$. Large magnetic curvature produced by the strong mirror field enhances the magnetic stress at the end of the FRC. Another point to notice is that the $R_m=2.8$ case has a larger magnetic field strength than the $R_m=1.2$ case, in the region near the right side of the *x-point* marked by bold-lined circles. In this region the strength of the mirror field is weakened by the edge pressure as for the weak mirror case of $R_m=1.2$. When $R_m=2.8$, there is a strong \mathbf{B} field in this region caused by the strong mirror field, in order to counteract the *edge-layer* plasma pressure. The magnetic stress becomes stronger due to the large magnetic curvature around the *x-point*, and consequently the ends of the FRC are sustained by the strong mirror field.

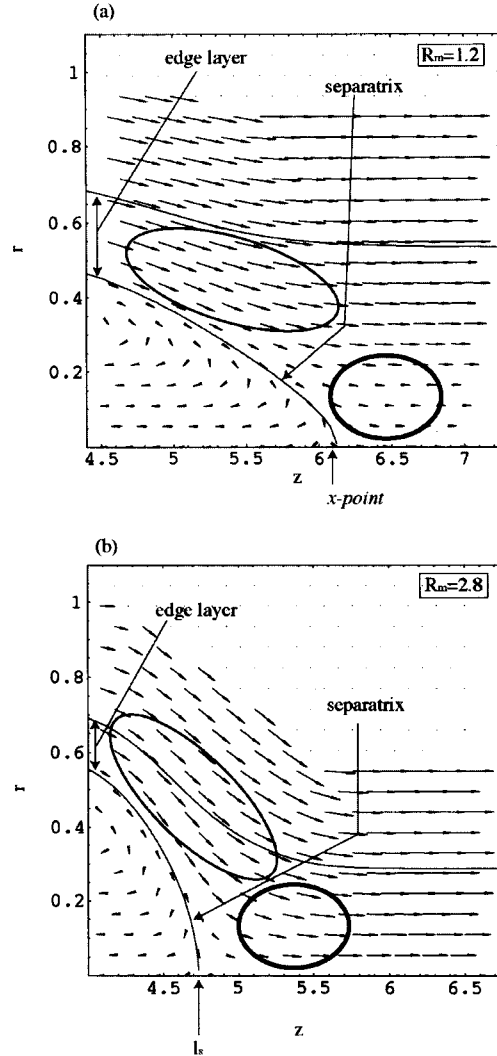


Fig. 4 The vector plot of the \mathbf{B} field near the end region of the FRC equilibrium with a thick *edge-layer* for $\gamma=15.0$. (a) $R_m=1.2$ and (b) $R_m=2.8$ case.

According to the above discussion, the reasons how the *edge-layer* pressure is supported by the mirror field and how the 2-D equilibrium is formed can be explained by considering the axial force balance. To calculate the axial force balance precisely with respect to numerical equilibria of this study, the calculation region for this is shown in Fig. 5. In this figure, $S_1 \sim S_5$ denote distinct regions for the surface integral. The pressure balance in its general form is given by

$$\begin{aligned}
 \nabla \cdot [\mathbf{T}_m - p\mathbf{I}] &= 0. \\
 \mathbf{T}_m &= \frac{1}{\mu_0} \left(\mathbf{B}\mathbf{B} - \frac{1}{2} B^2 \mathbf{I} \right). \quad (3)
 \end{aligned}$$

where p is the scalar pressure, \mathbf{I} is the unit tensor, and \mathbf{T}_m is the magnetic stress tensor. Neglecting the θ component, the integration is transformed into a surface integral using Gauss's theorem. The axial force balance is expressed by:

$$\int_{S_1} \left(-\frac{B_z^2}{2\mu_0} + p \right) dS + \int_{S_3} \frac{1}{\mu_0} \left(B_r B_z \cos \alpha + (B_z^2 - B_r^2) \sin \alpha \right) dS + \int_{S_1} \left(-\frac{B_z^2}{2\mu_0} - p \right) dS = 0, \quad (4)$$

$$\sin \alpha = \left(\sqrt{R_m} - 1 \right) / \sqrt{\left(\sqrt{R_m} - 1 \right)^2 + R_m (z_2 - z_1)^2},$$

$$\cos \alpha = \sqrt{R_m} (z_2 - z_1) / \sqrt{\left(\sqrt{R_m} - 1 \right)^2 + R_m (z_2 - z_1)^2}. \quad (5)$$

The effect of the magnetic curvature is contained in the second term on the left side of eq. (4). The mirror effect appears in the third term, and the edge effect is included in p of this term. The second term depends on $\sin \alpha$ and $\cos \alpha$ shown in eq. (5). If $R_m=1$ and $p=0$, $\sin \alpha$ and B_r on the surface S_3 is 0, so that the second term becomes 0, and eq. (4) reduces to Barnes relationship [2]. When $R_m=1$ and $p \neq 0$, the *edge-layer* pressure in the third term directly influences the force balance. When R_m is increased beyond 1, the second and the third terms of eq. (4) increase and contribute to the pressure balance along the axial direction. Thus $\psi=0$ surface, which tended to open up due to *edge-layer* pressure, remains closed by the effect of the strong mirror field. The numerical results shown in Sec. 3 are consistent with this interpretation.

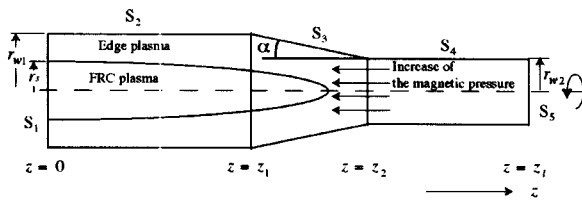


Fig. 5 A simple model for the axial force balance. Both the edge pressure and the mirror field are considered in this model. Symbols from S_1 to S_5 denote distinct regions for the surface integral.

5. Conclusion

The equilibrium calculation is performed for wide range of mirror ratio as $1.0 \leq R_m \leq 2.8$. The effects of the *edge-layer* pressure for varying thickness of *edge-layer* are examined for each mirror ratio by scanning the parameter γ . The region in which closed $\psi=0$ surface equilibria exist is obtained for the parameter range $0.1 < \delta < 0.37$ and $1 < R_m < 2.8$ due to the calculation. It is found that the critical value of δ_c increases from 0.2 to 0.37 as the mirror ratio increases from 1 to 1.6 in the weak mirror case. A mirror ratio in the range from 1.6 to 2.0 is required to sustain the equilibrium for a thick *edge-layer* of $\delta \sim 0.37$. These numerical results can be explained with an axial force balance calculation. A simple model of axial force balance, which takes both the edge and the mirror effects into consideration, shows that the curvature of the magnetic field near the *x-point* is enhanced by the strong mirror field. A sufficiently strong mirror field extends the region in which equilibrium solutions exist to the case of a thick *edge-layer*.

References

- [1] M. Tuszewski, Nucl. Fusion **28**, 2033 (1988).
- [2] W.T. Armstrong *et al.*, Phys. Fluids **24**, 2068 (1981).
- [3] M. Tuszewski, Plasma Phys. Control. Fusion **26**, 991 (1984).
- [4] R.L. Spencer and M. Tuszewski, Phys. Fluids **28**, 1810 (1985).
- [5] K. Suzuki, J. Phys. Soc. Jpn. **54**, 2155 (1985).
- [6] D.W. Hewett and R.L. Spencer, Phys. Fluids **26**, 1299 (1983).
- [7] S. Okada, Y. Kiso, S. Goto and T. Ishimura, J. Appl. Phys. **65**, 4625 (1989).
- [8] M. Tuszewski and R.K. Linford, Phys. Fluids **25**, 765 (1982).
- [9] A.L. Hoffman and R.D. Milroy, Phys. Fluids **26**, 3170 (1983).
- [10] L.C. Steinhauer, Phys. Fluids **29**, 3379 (1986).
- [11] H. Himura, S. Okada, S. Sugimoto, and S. Goto, Phys. Plasmas **2**, 191 (1995).
- [12] T. Ohtsuka, M. Okubo, S. Okada and S. Goto, Phys. Plasmas **5**, 3649 (1998).
- [13] Y. Suzuki, S. Okada, and S. Goto, Phys. Plasmas **7**, 4062 (2000).
- [14] J.W. Cobb, T. Tajima, and D.C. Barnes, Phys. Fluids B **5**, 3227 (1993).
- [15] K. Suzuki, J. Phys. Soc. Jpn. **55**, 158 (1986).